Sciencexpress Report

RNA Editing Underlies Temperature Adaptation in K^+ Channels from Polar Octopuses

Sandra Garrett[1] and Joshua J.C. Rosenthal[1,2*]

[1]Institute of Neurobiology, University of Puerto Rico–Medical Sciences Campus, San Juan 00901, Puerto Rico. [2]Department of Biochemistry, University of Puerto Rico–Medical Sciences Campus, San Juan 00936, Puerto Rico.

*To whom correspondence should be addressed. E-mail: rosenthal.joshua@gmail.com

To operate in the extreme cold, ion channels from psychrophiles must have evolved structural changes to compensate for their thermal environment. A reasonable assumption would be that the underlying adaptations lie within the encoding genes. Here we show that delayed rectifier K^+ channel genes from an Antarctic and a tropical octopus encode channels that differ at only four positions and display very similar behavior when expressed in *Xenopus* oocytes. However, the transcribed mRNAs are extensively edited, creating functional diversity. One editing site, which recodes an isoleucine to a valine in the channel's pore, greatly accelerates gating kinetics by destabilizing the open state. This site is extensively edited in both Antarctic and Arctic species, but mostly unedited in tropical species. Thus A-to-I RNA editing can respond to the physical environment.

Action potentials, during which the electrical potential across a cell membrane rapidly rises and falls, are the nervous system's basic unit of communication. In 1949 Hodgkin and Katz, using the squid giant axon, showed that the action potential's falling phase has steeper temperature dependence than the rising phase and that the membrane's return to the resting potential is particularly sensitive to temperature (*1*). Accordingly, they hypothesized that ectotherms would be forced to regulate the waveform of their action potentials to accommodate the thermal environment. As it emerged that the rising phase was due to voltage-dependent Na^+ channels, and the falling phase to voltage-dependent K^+ channels (*2*) (*3*), the early observations suggested that potassium channel gating is more temperature sensitive than sodium channel gating. This assertion has since been demonstrated (*4*). These observations also suggested that the closing kinetics of potassium channels, which determine the rate of return to rest, should be especially temperature sensitive, and this has also been shown (*5*). If K^+ channel kinetics did not adapt to temperature, the cold would make action potentials disproportionately broad and severely limit repetitive firing. Accordingly, potassium channel kinetics should be a prime target for regulation in organisms adapted to the extreme cold. This study shows that they are, but by an unsuspected mechanism.

To identify mechanisms of cold adaptation, we compared potassium channel orthologs from a tropical and an Antarctic octopus. Despite the enormous body of work on squid axons, we chose octopus as a comparative model because individuals generally have small home ranges, and species inhabit widely different thermal environments, from the poles to the equator. The Antarctic octopus was a *Pareledone sp*., which was collected from McMurdo Station (6), where the waters, at -1.8ºC, are in equilibrium with sea ice, and have been so for the last 28 to 38 million years (*7*). For comparison we used *Octopus vulgaris* which we collected from a Puerto Rican reef at 30ºC. Over the year, the temperature at this location fluctuates between ~25ºC and 35ºC. We sequenced the ortholog of the squid delayed rectifier from each species (*8*).

Based on conventional natural selection, we hypothesized that the channels' genes would have evolved mutations to help tune them to their respective environments. Suprisingly, the primary sequences encoded by the two genes were virtually identical, differing at only four positions (fig. S1). They also shared 95% identity with the widely studied *Loligo* ortholog, indicating that the basic genetic template for the delayed rectifier is remarkably similar in coleoid cephalopods. To test whether the four differences affected function, each channel was expressed in *Xenopus* oocytes and characterized electrophysiologically at 2, 15 and 25°C. Experiments focused on opening and closing kinetics, which are the most temperature sensitive properties, but also on the

voltage dependence of opening and the rate of inactivation. Functionally, the two channels were virtually identical (Fig. 1A and table S1). As with the squid delayed rectifier, they opened rapidly in response to depolarization and exhibited a steep voltage-dependence between -20 mV and 20 mV. Upon repolarization, they closed quickly, following a simple exponential time course. When held at a constant depolarizing potential, both channels inactivated slowly, over the course of several seconds. There were some subtle differences. Antarctic channels opened slightly faster (Fig. 1A), but this difference was only significant at potentials near the threshold for activation. The steepness factor (Z) of their steady-state voltage dependence was also slightly smaller (table S1). Overall though, in spite of their drastically different environments, the genomically encoded channels displayed essentially the same behavior. At their respective native temperatures, Antarctic channels would open about 14 times slower, and close about 60 times slower, than tropical channels (see Q_{10}'s in table S1). Either the Antarctic octopus barely compensates for the cold, or post-transcriptional mechanisms are important.

Adenosine deamination, the most common form of RNA editing, is carried out by a family of enzymes known as ADARs (Adenosine Deaminases that Act on RNA). ADARs convert adenosine (A) to inosine (I) (*9*). Because inosine is read as guanosine by the translational machinery, codons in mRNAs can change (*10*). A to I editing is common in the nervous system, having been identified in mRNAs encoding ion channels and receptors (*11-13*). Extensive editing by this mechanism has been described in squid, where it modifies diverse mRNAs, including the squid delayed rectifier K^+ channel (*14, 15*). We compared cDNA sequences to check whether the octopus channels were edited as well. Our preliminary cloning results showed site specific A/G variation in the electropherograms of direct sequences, a hallmark of A-to-I RNA editing. To investigate further, we cloned and sequenced 50 individual cDNAs from the stellate ganglia of each species and then looked for A or G variation that was not present in the gene sequence. Each species showed extensive editing. For the Antarctic octopus, there were 18 editing sites, nine of which caused amino acid changes (fig. S1). For the tropical octopus, there were 15 editing sites, ten of which caused amino acid changes. Of the 12 non-silent sites, five were species specific and four of the shared sites were edited to significantly different extents (Fig. 2A). Thus in these channels greater species diversity is generated by RNA editing than by gene mutations.

Do the RNA edits alter channel function? Four editing sites were selected for further study because they were edited exclusively, or to a much greater extent, in one species or the other; N105G and I321V were considered candidates for cold adaptation, while N40S and S54G were considered candidates for warm adaptation. N105G is only found in the Antarctic channel and N40S is only found in the tropical channel. The other two sites showed greater than 50% differences in editing, with I321V highly edited in the Antarctic channel and S54G highly edited in the tropical channel (Fig 2A). I321V lies in the fifth transmembrane span, (S5) within the pore domain (Fig. 2B) (*16*). The rest of the sites are located in the T1 domain (Fig. 2B), a region important for tetramerization (*17, 18*). At the genomic level, all of these positions except S54G are nearly invariant among Kv1 channels, suggesting that they are functionally important.

To characterize their effects, each of the four edits were singly introduced into the unedited channel background (genomic) and studied at 15 and 25°C. Three of the four editing sites produced clear functional changes to a number of channel properties (table S1). The tropical edits, (N40S and S54G), had similar effects: both slowed channel opening by about 50%, and both increased the rate of inactivation, by 30% for N40S and by 60% for S54G (fig. S2). These effects on gating were somewhat surprising, given that both sites are in the cytoplasmic tetramerization domain, thought to be physically separate from the membrane-bound voltage sensor and pore (*16, 19*). However, others have reported that the T1 domain influences function (*20, 21*). The Antarctic edits also altered function. N105G caused subtle changes in activation and deactivation kinetics. The most pronounced effect of all, however, was due to I321V, which more than doubled the rate of closure (Fig. 1B and C) and produced a positive shift in the voltage dependence of opening (table S1). This effect was dominant, speeding closing when combined with other editing sites that mimicked natural editing patterns (Supporting Online Material, table S1 and fig. S3).

Since I321V was highly edited in the Antarctic species and dramatically accelerated deactivation kinetics, which underlie the action potential's afterhyperpolarization, it was a good candidate for cold adaptation. This position lies in the S5 helix, an interface between the voltage sensor and the ion conduction pathway (*16, 22, 23*). At negative voltages, the voltage sensor is thought to force the gate shut via contact between the S4-S5 linker and the S6 helix. At positive potentials, the voltage sensor moves away, allowing the channel to open (*22, 24, 25*). The open state is not stable, however, and channels flicker between open and closed conformations (*26, 27*). Because I321V causes the channel to close faster and also shifts its voltage sensitivity to more positive potentials, we hypothesized that it destabilizes the open state. This possibility was examined directly by recording single channel events. Representative records for both unedited and I321V Antarctic channels show that I321V channels close more frequently (Fig. 3A and C). To quantify this phenotype, recordings were idealized using an algorithm and the durations of open and closed events were determined

(*28*). The average open duration for the unedited Antarctic channels was twice that of I321V channels. The durations of closed events did not change, suggesting that I321V selectively affects the open to closed state transition. This idea was reinforced by a simple 5 state model (Fig. 3E and F): by doubling the backwards rate constant for the final transition, both the macroscopic difference in closing kinetics (Fig. 3E and F), and the single channel difference in open duration (Fig. 3G and H), could be recapitulated. In agreement with experimental data, the model predicts nearly identical activation kinetics and open probability for the two channels (Fig 3E and F). Thus it appears that once open, I321V channels are poised to close rapidly, but the opening kinetics and other properties are preserved. In an axon, we predict that the major effect of I321V channels would be to accelerate the afterhyperpolarization, and thus shorten the refractory period, increasing repetitive firing rates.

If editing of codon I321 is indeed a cold adaptation, then we might expect other cold adapted octopuses to make the same edit. To test this idea, we collected two Arctic species from benthic trawls northwest of the Svalbard archipelago, where water temperatures at ~ 0°C were similar to those in Antarctica. We also collected two more tropical species, one from Puerto Rico and one from a desert lagoon in Baja California, and two temperate species from California (Fig. 4A). Editing levels at I321V, as determined by a primer extension assay, correlated very well with the environmental temperature where the species were captured (Fig. 4B and C). We also quantified all editing sites in the six new species using direct sequencing. Although many of the other editing sites were edited differentially among the eight species, I321V correlated most closely with temperature (table S2).

In Coleoid Cephalopods, and in other higher metazoans, A-to-I RNA editing adds a layer of complexity to the proteome. A clear advantage to this strategy is that it allows options: different isoforms can be expressed in response to different conditions. Exactly how organisms exercise these options is largely unknown. Drosophila and rodents use editing to fine tune protein function temporally, over the course of development (*29, 30*) and spatially, in different brain regions (*12*). Here we present evidence that RNA editing can respond to an external pressure: temperature. While still maintaining the basic K^+ channel plan, octopus can make fast closing versions, and the extent of their expression can be graded. A basic question that remains is whether octopuses use editing for rapid acclimation or long-term adaptation. For each possibility, the biochemical mechanisms that impart temperature sensitivity to the editing process would be different. Others have shown that the RNA structures that drive editing evolve and generate species-specific patterns, suggesting a plausible mechanism for adaptation (*31*). Acclimation could arise from temperature sensitive RNA structures, or temperature-dependent expression of other factors that control ADAR's access to specific editing sites.

References and Notes

1. A. L. Hodgkin, B. Katz, *J Physiol* **109**, 240 (Aug, 1949).
2. A. L. Hodgkin, A. F. Huxley, *J Physiol* **116**, 449 (Apr, 1952).
3. C. M. Armstrong, F. Bezanilla, E. Rojas, *J Gen Physiol* **62**, 375 (Oct, 1973).
4. F. Kukita, *J Membr Biol* **68**, 151 (1982).
5. B. M. Rodriguez, D. Sigg, F. Bezanilla, *J Gen Physiol* **112**, 223 (Aug, 1998).
6. Materials and methods are available as supporting material on *Science* Online.
7. M. E. Katz *et al.*, *Science* **332**, 1076 (May 27).
8. J. J. Rosenthal, R. G. Vickery, W. F. Gilly, *J Gen Physiol* **108**, 207 (Sep, 1996).
9. B. L. Bass, H. Weintraub, *Cell* **55**, 1089 (Dec 23, 1988).
10. C. Basilio, A. J. Wahba, P. Lengyel, J. F. Speyer, S. Ochoa, *Proc Natl Acad Sci US A* **48**, 613 (Apr 15, 1962).
11. T. Bhalla, J. J. Rosenthal, M. Holmgren, R. Reenan, *Nat Struct Mol Biol* **11**, 950 (Oct, 2004).
12. C. M. Burns *et al.*, *Nature* **387**, 303 (May 15, 1997).
13. T. Melcher, S. Maas, M. Higuchi, W. Keller, P. H. Seeburg, *J Biol Chem* **270**, 8566 (Apr 14, 1995).
14. D. E. Patton, T. Silva, F. Bezanilla, *Neuron* **19**, 711 (Sep, 1997).
15. J. J. Rosenthal, F. Bezanilla, *Neuron* **34**, 743 (May 30, 2002).
16. S. B. Long, E. B. Campbell, R. Mackinnon, *Science* **309**, 897 (Aug 5, 2005).
17. A. Kreusch, P. J. Pfaffinger, C. F. Stevens, S. Choe, *Nature* **392**, 945 (Apr 30, 1998).
18. M. Li, Y. N. Jan, L. Y. Jan, *Science* **257**, 1225 (Aug 28, 1992).
19. W. R. Kobertz, C. Williams, C. Miller, *Biochemistry* **39**, 10347 (Aug 29, 2000).
20. S. J. Cushman *et al.*, *Nat Struct Biol* **7**, 403 (May, 2000).
21. D. L. Minor *et al.*, *Cell* **102**, 657 (Sep 1, 2000).
22. Z. Lu, A. M. Klem, Y. Ramu, *J Gen Physiol* **120**, 663 (Nov, 2002).
23. G. J. Soler-Llavina, T. H. Chang, K. J. Swartz, *Neuron* **52**, 623 (Nov 22, 2006).
24. S. B. Long, X. Tao, E. B. Campbell, R. MacKinnon, *Nature* **450**, 376 (Nov 15, 2007).
25. M. M. Pathak *et al.*, *Neuron* **56**, 124 (Oct 4, 2007).
26. F. Conti, E. Neher, *Nature* **285**, 140 (May 15, 1980).
27. I. Llano, C. K. Webb, F. Bezanilla, *J Gen Physiol* **92**, 179 (Aug, 1988).
28. F. Qin, L. Li, *Biophys J* **87**, 1657 (Sep, 2004).
29. B. R. Graveley *et al.*, *Nature* **471**, 473 (Mar 24, 2011).
30. H. Lomeli *et al.*, *Science* **266**, 1709 (Dec 9, 1994).

31. R. A. Reenan. Nature **434**, 410 (Mar 17, 2005).
32. E. R. Liman, J. Tytgat, P. Hess, *Neuron* **9**, 861 (Nov, 1992).
33. M. Taglialatela, L. Toro, E. Stefani, *Biophys J* **61**, 78 (Jan, 1992).
34. L. S. Milescu, G. Akk, F. Sachs, *Biophys J* **88**, 2494 (Apr, 2005).
35. L. M. Roberson, J. J. Rosenthal, *RNA* **12**, 1907 (Oct, 2006).

Acknowledgments: We are grateful to Thomas de Lange Wenneck and the Norwegian Institute of Marine Research for the invitation to collect Arctic cephalopods aboard the RV *Jan Mayen*. We thank Dr. Chris DeVries for samples of *Pareledone*. This work was supported by the National Institutes of Health (NIH) Ruth L. Kirschstein National Research Service Predoctoral Fellow Award FNS064774A, NIH 2 U54 NS039405-06, NIH R01 NS064259NIH, and the National Science Foundation (NSF) IBN-0344070. Part of the work was conducted in the Molecular Biology Core Facility at the Institute of Neurobiology that is supported by RCMI Grant #G12 RR 03051. Kv1 sequences have been submitted to genbank. The accession numbers are as follows: JQ246406 - Pareledone sp., JQ246407 - Octopus vulgaris, JQ246408 - Octopus digueti, JQ246409 - Octopus defilippi, JQ246410 - Octopus bimaculata, JQ246411 - Bathypolypus arcticus, JQ246412 - Benthoctopus piscatorum, JQ246413 - Octopus rubescens. SCG performed all experiments, participated in designing experiments, collected Arctic samples, and wrote the manuscript. JJCR participated in designing experiments, collected Antarctic, temperate, and tropical samples, and edited the manuscript.

Supporting Online Material

www.sciencemag.org/cgi/content/full1212795/DC1
Materials and Methods
Figs. S1 to S3
Tables S1 to S3
References (*32–35*)

17 August 2011; accepted 9 December 2011
Published online 5 January 2012; 10.1126/science.1212795

Fig 1. RNA editing, but not gene level differences, change channel function. A, Current traces for Antarctic and tropical K_v1 genomic channels in response to a voltage step from -80 mV to +60 mV. Traces have been scaled in order to show the near identity in opening and closing kinetics. B, Representative current traces focusing on closing kinetics for genomic Antarctic and I321V edited channels. Currents were activated by a stimulus to +50 mV, but only their decay following a return to -80 mV is shown. C, Channel closing kinetics over a range of repolarization voltages following an activating step to +50 mV. Error bars = s.e.m; n = 16 for genomic and 9 for I321V. ◆ = genomic Antarctic and ■ = I321V edited. All data was recorded from voltage clamped *Xenopus* oocytes injected with cRNA for the appropriate construct and the temerparature was maintained at 15°C.

Fig 2. mRNAs encoding octopus $K_v1$channels are extensively edited. A, Editing percentages for the 12 non-silent sites found in the Antarctic and tropical octopus Kv1 channels calculated by sequencing 50 individual cDNA clones for each channel. B, Octopus editing sites occur in different functional domains. Homologous positions to those altered by RNA editing in octopus Kv1 channels, shown in red, have been mapped on the $K_v1.2$ crystal structure(*23*). One full subunit of the tetramer is shown (blue); for the pore region, all four subunits are shown, each in a different color.

Fig 3. The editing site I321V speeds channel closing kinetics by destabilizing the open state. Current traces from cell-attached patches containing single Antarctic genomic (A) and I321V (C) Kv1 channels. Channels opened in response to a voltage step from -80 mV to +60 mV. I321V channels close more frequently. Overlapping red lines (insets) show idealizations of traces as a series of open and closed events. B and D, Duration distributions of open events for genomic Antarctic and I321V channels. The average duration of open events in the genomic channel (3.42 ms) was about twice that of I321V channels (1.72 ms). E and F, Simple 5 state models for genomic Antarctic and I321V channel gating and simulations generated from the models. Doubling the backwards rate constant for the final transition recapitulates both the macroscopic difference in closing kinetics and the single channel behavior (G and H) between genomic and I321V channels. Rate constants were assumed to depend exponentially on voltage: $k = k_0 e^{(zFV/RT)}$ where F is the Faraday's constant, V is voltage, R is the universal gas constant, and T is the temperature. For the above models: k_{1f} = 700, z = 0.3; k_{1b} = 50, z = 1.6; k_{2f} = 1200, z = 1.8; k_{2b} = 25, z = 1.1; k_{3f} = 600, z = 0.8; k_{3b} = 150, z = 1.5; k_{4f} = 3000, z = 0.02; k_{4b} variable, z = 0.2. A stochastic simulation of 1000 channels pulsed from -80mV to +60mV and back to -80mV showed faster closing with the I321V model. The maximum open probability was similar: 0.59 vs. 0.55 for genomic and I321V, respectively. Closing rates (single exponential fit, overlapping red line) were similar to those obtained from room temperature experimental data: 625 and 1250 (s^{-1}) simulated kinetics vs. 610 and 1423 (s^{-1}) experimental kinetics for genomic and I321V, respectively. For the single channel simulations, the average open duration using the I321V model was half that for the genomic model.

Fig 4. The extent of editing at I321V correlates with the water temperature where octopus species were captured. A,

Collection sites for eight octopus species and the water temperatures and habitats at the time of capture. B, representative poison primer extension assay showing the amount of I321V editing among the eight species. D, I321V editing percentages for the eight species, based on poison primer extension assays, versus water temperature at capture site. Error bars = SEM; $n = 4$.

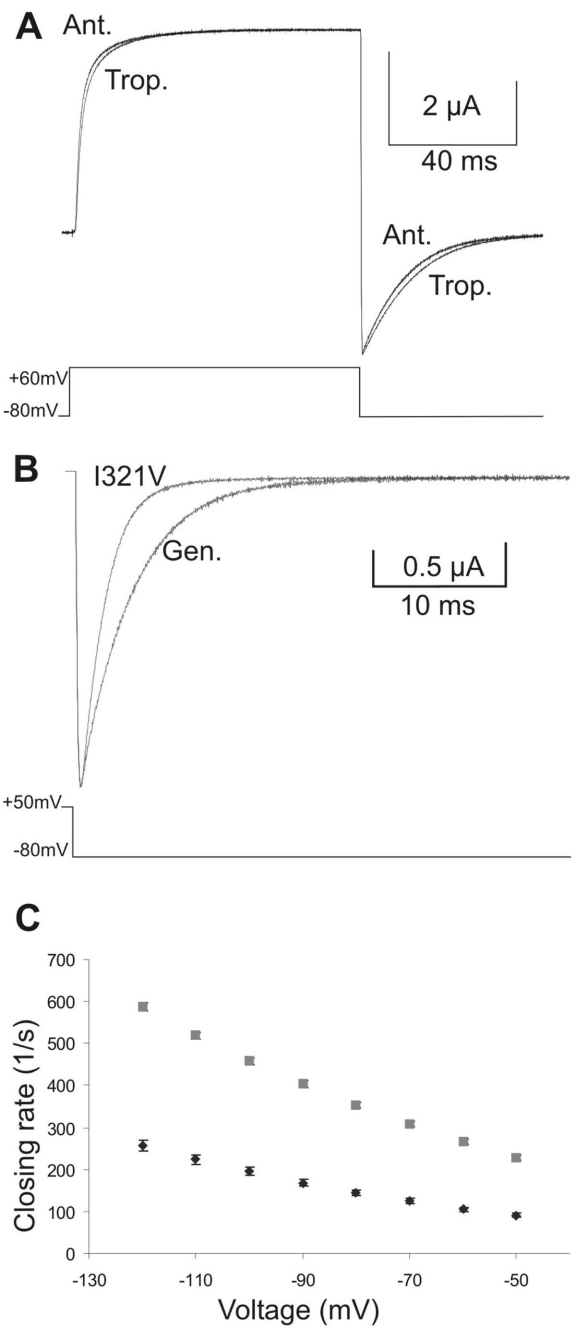
A
Ant.
Trop.
2 µA
40 ms
Ant.
Trop.
+60mV
-80mV
B
I321V
Gen.
0.5 µA
10 ms
+50mV
-80mV
C
Closing rate (1/s)
700
600
500
400
300
200
100
0
-130
-110
-90
-70
-50
Voltage (mV)

A

Site	Nuc. #	Amino acid change	Domain	Editing percentages	
				Antarctic	Tropical
1	119	N40S	T1	0	76
2	124	S42G	T1	0	10
3	160	S54G	T1	10	68
4	175	T59A	T1	0	10
5	314-315	N105G	T1	92	0
6	348	K116R	T1	16	0
7	379	K127E	T1	88	78
8	403	I135V	T1	96	80
9	499	I167V	S1	96	78
10	508	M*170V	S1	98	84
11	961	I321V	S5	92	30
12	1114	I372V	P/S6	90	82

B

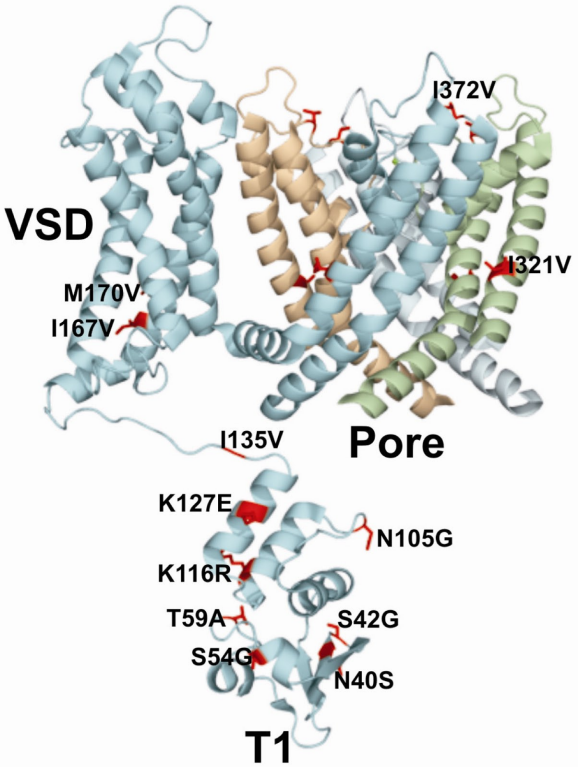

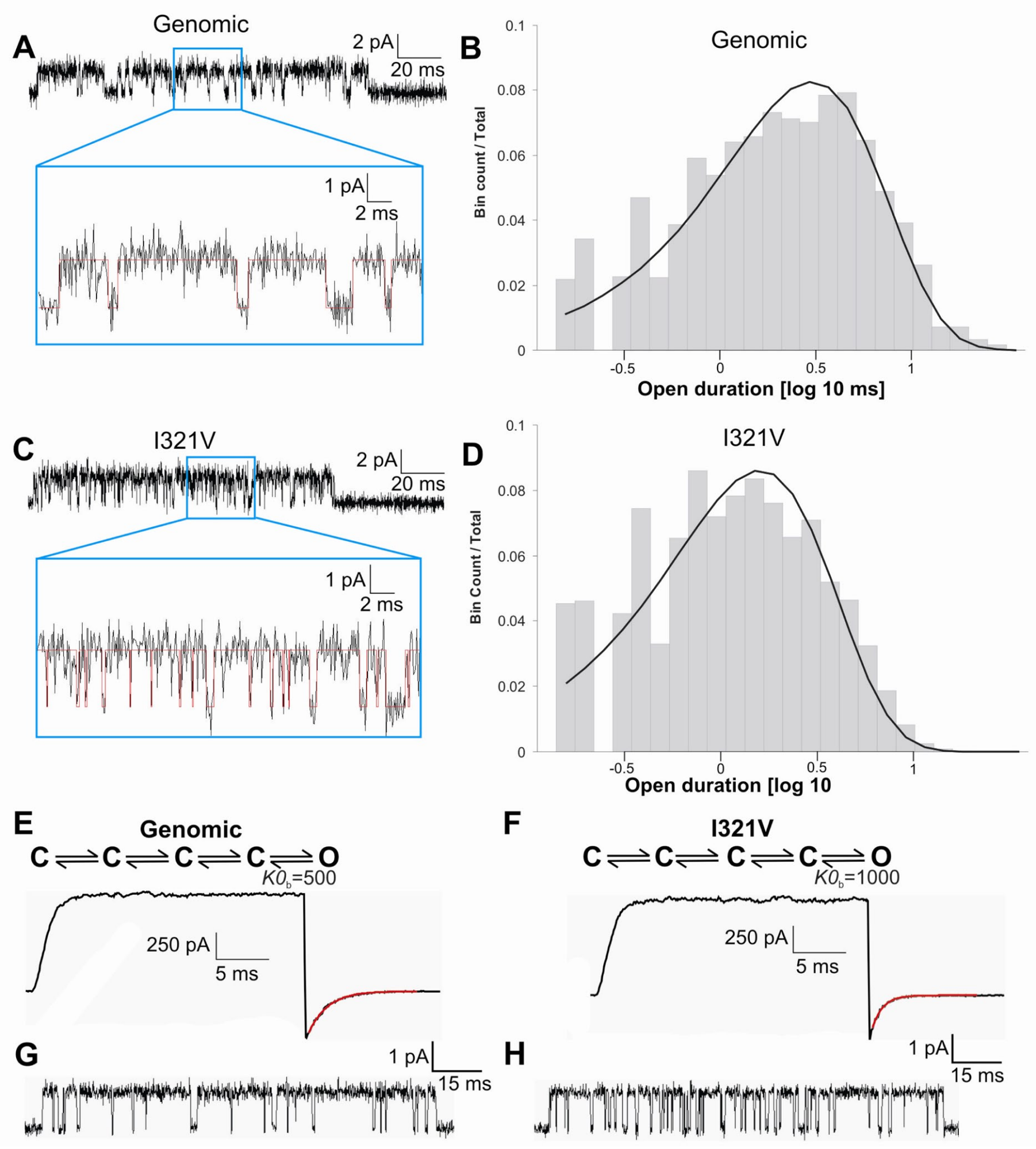
A
Genomic
2 pA
20 ms
1 pA
2 ms
B
Genomic
Bin count / Total
0.1
0.08
0.06
0.04
0.02
0
-0.5
0
0.5
1
Open duration [log 10 ms]
C
I321V
2 pA
20 ms
1 pA
2 ms
D
I321V
Bin Count / Total
0.1
0.08
0.06
0.04
0.02
0
-0.5
0
0.5
1
Open duration [log 10
E
Genomic
C ⇌ C ⇌ C ⇌ C ⇌ O
K0b=500
250 pA
5 ms
F
I321V
C ⇌ C ⇌ C ⇌ C ⇌ O
K0b=1000
250 pA
5 ms
G
1 pA
15 ms
H
1 pA
15 ms

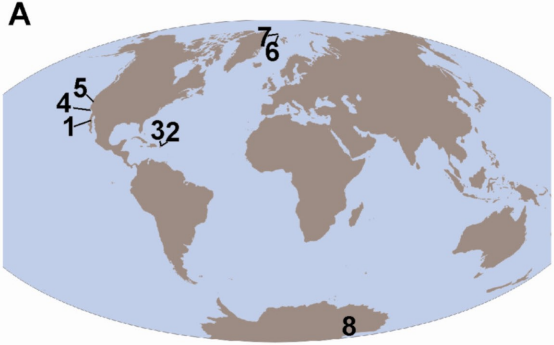

Editing percentages at site I321V for eight octopus species

	Species	Collection site	Water temp. (°C)
1	*Octopus digueti*	Estuary, Baja California	37
2	*Octopus defilippi*	Reef flat, Rio Grande, PR	32
3	*Octopus vulgaris*	Inshore reef, Luquillo, PR	28
4	*Octopus bimaculata*	Near shore rock ledge, Catalina Is., CA	18
5	*Octopus rubescens*	Near shore, Monterey, CA	10
6	*Benthoctopus piscatorum*	Benthic trawl, north Svalbard, Norway	0
7	*Bathypolypus arcticus*	Benthic trawl, north Svalbard, Norway	-1
8	*Pareledone sp.*	McMurdo station, Antarctica	-2

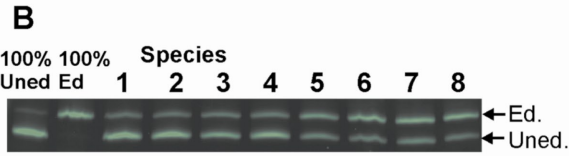

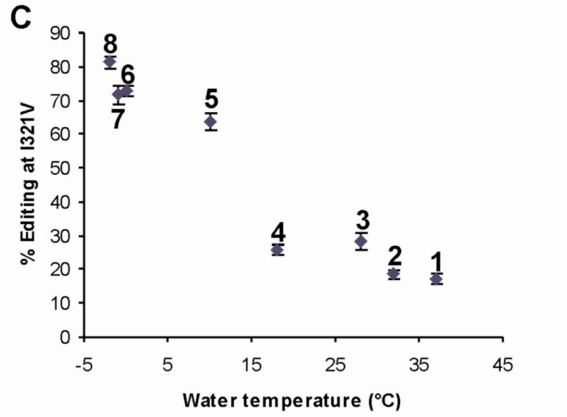

www.sciencemag.org/cgi/content/full/science.1212795/DC1

Supporting Online Material for

RNA Editing Underlies Temperature Adaptation in K^+ Channels from Polar Octopuses

Sandra Garrett and Joshua J. C. Rosenthal*

*To whom correspondence should be addressed. E-mail: rosenthal.joshua@gmail.com

Published 5 January 2012 on *Science* Express
DOI: 10.1126/science.1212795

This PDF file includes:

Materials and Methods

Octopus collection. *Pareledone* sp. was collected from waters off McMurdo station, Antarctica. The two Arctic specimens, *Bathypolypus arctiucs* and *Benthoctopus piscatorum*, were collected from benthic trawls northwest of the Svalbard archipelago, Norway, at a depth of approximately 1000 m. *Octopus vulgaris* was collected from an inshore reef off Luquillo, Puerto Rico. *Octopus defilippi* was collected from a tidal pool near Rio Grande, Puerto Rico. *Octopus digueti* was collected from San Lucas cove, near Santa Rosalia, Baja California Sur. *Octopus bimaculata* was collected near Bird Rock, just off Two Harbors, Catalina Island, California, USA. *Octopus rubescens* was collected from a reef off Monterey, California, USA. All specimens were adults. Specimens were dissected immediately after collection; the stellate ganglia were cleaned of connective tissue, removed, and preserved in RNA later solution (Ambion, Austin TX) for later RNA extraction and cDNA synthesis. A sample of gill tissue was placed in silica desiccant in order to preserve it for later genomic DNA extraction.

Cloning and mapping editing sites. To isolate the delayed rectifier Kv1 channel from octopus, degenerate nested primers (Table S3, primers 1-3) were designed based on an alignment of K_v1 sequences from 20 different species, and used to amplify a ~300 bp fragment from *O. vulgaris* and *Pareledone* sp. cDNA with Phusion DNA polymerase (New England Biolabs, Ipswich, MA). Non-degenerate primers (Table S3, primers 4-7) were then designed based on the sequence of the 300 bp fragment and were used to amplify the 5' and 3' ends using a RACE protocol (Clontech Smart RACE kit, Mountain View, CA). These primers also worked for *O. digueti*,. Full-length cDNA's were then

isolated using primers, based on the RACE sequences, from the 5' start codon and just downstream from the 3' stop codon (Table S3, primers 8-13). 50 individual clones of full-length K_v1 cDNAs were sequenced for each species. Because the position of the squid K_v1 gene's single intron was conserved in octopus, the gene sequence was easily amplified using genomic DNA from the same specimens (Table S3, primer 14 with species-specific R primer). The 50 clones and the genomic K_v1 sequence were aligned and compared to identify sites of A/G variation. If a particular position had an A in the genomic sequence and a G in at least 3 of the 50 cDNA clones, it was considered an editing site. The sequences of the Kv1 channels for all species used in this study will be furnished to Genbank upon acceptance.

Mutagenesis and functional expression. To characterize the *O. vulgaris* and *Pareledone* sp. genomic channels, fully unedited clones were selected and prepared for expression. The coding sequence was amplified with primers that added a Kozak sequence upstream from the start codon and introduced BglII sites at both ends (Table S3, primers 15-17). Products were cloned and sequenced to confirm that no errors had been introduced and then subcloned into pBSTA, a plasmid vector designed to generate cRNA for high-level expression in *Xenopus* oocytes (*32*). Single edit constructs were generated by subcloning the appropriate fragment from an edited cDNA clone. The N105G and I321V single edits were ligated into the *Pareledone* sp. genomic background, while the N40S and S54G single edits were ligated into the *O. vulgaris* genomic background. The editing combination (PspEP11, OvEP9, and PspEP0) constructs were made by a similar approach. The plasmids were then used as template for RNA synthesis

(Epicentre mScript mRNA kit, Madison, WI). 36.8 nl of RNA was injected per oocyte. RNA concentrations, which varied from 5-100 ng/ul, were titrated in order to maximize oocytes expressing from 1-10 A current. Oocytes were incubated at 18 C.

Electrophysiology. Experiments were performed 2 - 3 days post-injection using a cut-open oocyte vaseline gap voltage clamp setup (*33*) and chamber temperatures were controlled at either 2, 15 or 25 C. Saponin (0.5% in internal solution) was used to gain electrical access to the oocyte's interior. The saponin solution was then rinsed away and replaced with an internal solution (120 mM K^+-methanesulfonic acid (MES), 5 mM EGTA, 10 mM HEPES, pH 7.5). The external bath solution contained 20 mM K-MES, 100 mM N-methylglucamine (NMG)-MES, 2 mM $CaCl_2$, 1 mM $MgCl_2$, and 10 mM HEPES (pH 7.5). The internal voltage electrode (resistance = 0.2 - 0.5 MΩ) was filled with 1 M KCl. Bridges were filled with 3% agarose in 3M K-MES. Temperature in the external bath was maintained constant with a feedback temperature controller and peltier devices, and was independently verified to be within 0.8 C of the target temperature before the start of each experiment. Voltage-clamp protocols were controlled with a Dagan Clampator One oocyte clamp. Analog signals were sampled at 100 kHz and filtered at 10 kHz and leak subtraction done with a P/4 protocol. Resting potential was maintained at -80 mV and voltage protocols were as follows: for activation they were -50 to +80 in 10 mV steps, for; deactivation they were first activated by a pulse to +50mV then stepped from -120 to 0 in 10 mV steps, and for inactivation they were - to +50. Pulse durations varied depending on the temperature at which experiments were conducted.

Data analysis was performed using the Analysis program (kindly provided by F. Bezanilla). Voltage-dependence of conductance, half time of activation ($T_{1/2}$), rate of channel closing, and τ of slow inactivation (Table S1) were determined for all edited and unedited channels. The time constant of deactivation was determined by fitting a single exponential to the tail currents. For activation kinetics, the time required for the current to reach 1/2 of its maximum amplitude was recorded at each voltage. From the same records, relative conductance was estimated by measuring the peak tail currents produced by each test pulse. Plots of relative conductance vs. voltage were then fit with a two-state Boltzmann equation: $I/I_{max} = (1 + e^{-ZF(V-V_{1/2})RT})^{-1}$ where I/I_{max} is the normalized tail current amplitude, Z is the effective charge or steepness factor, $V_{1/2}$ is the voltage of half activation, F is the Faraday constant, R is the universal gas constant, and T is the temperature. For inactivation, currents resulting from long duration voltage steps were fitted with a single exponential to obtain the time constant.

Single channel recordings were made with cell attached patches. Oocytes were placed in a bath of internal solution (110 mM K^+-aspartate, 10 KCl, 2.5 EGTA, 0.5 MgCl2, and 10 HEPES). The patch electrode (resistance = 3 – 7 MΩ) contained an external solution (100 mM NMG-MES, 20 KCl, 2 $CaCl_2$, 1 $MgCl_2$, and 10 HEPES). Experiments were conducted at room temperature (25°C). Voltage-clamp protocols were controlled using an Axopatch 200B patch clamp. Analog signals were sampled at 14 kHz and filtered at 5 kHz. Resting potential was -80 mV. Patches were stepped to various potentials for 200 ms every 5 s. Data presented in this paper was derived from steps to +60 mV, however

results from different potentials were not qualitatively different. To subtract leak and capacitive current, traces with no open events were fit with a double exponential, and this fit was subtracted from traces which contained single events.

Data analysis of single channel recordings was done with QuB software (QuB, New York State University, Buffalo, NY). Single channel recordings were idealized as a series of open and closed events. The durations of the open and closed events were then binned logarithmically and the distributions and average durations determined for each. Durations were determined using idealized single channel data from 5-6 patches; in each patch, between 10 and 20 200 ms traces were analyzed. To arrive at a five state model for channel activation, the rate constants for the final transition were derived from single channel data. The rate constants for all other transitions were based on fits to macroscopic data. Rate constants were then fine-tuned to fit both data sets (*28, 34*). The I321V and genomic models were then used to simulate both macroscopic currents and single channel currents.

Poison primer extension assay. I321V editing was quantified in eight octopus species using a poison primer extension assay which has been described in detail (*35*). Briefly, the Kv1 channel (full ORF, see Table S3, primers 20-21) was amplified from stellate ganglia cDNA and used as a template for the extension assay. Acyclo TTP was used as a terminator. A 5' hexachloroflourescein labeled primer was used to initiate extension (Table S3, primers 18-19) and bound 11 bp downstream from I321V. Gels were scanned using a Typhoon 9200 fluorescence imager using a 532 nm laser and a 555 nm BP20

filter. Signals were analyzed using ImageQuant software (Amersham Biosciences, Piscataway, New Jersey) and corrected for run through as described (*35*). The edited extension product was 4 bp larger than the unedited product.

Fig. S1.

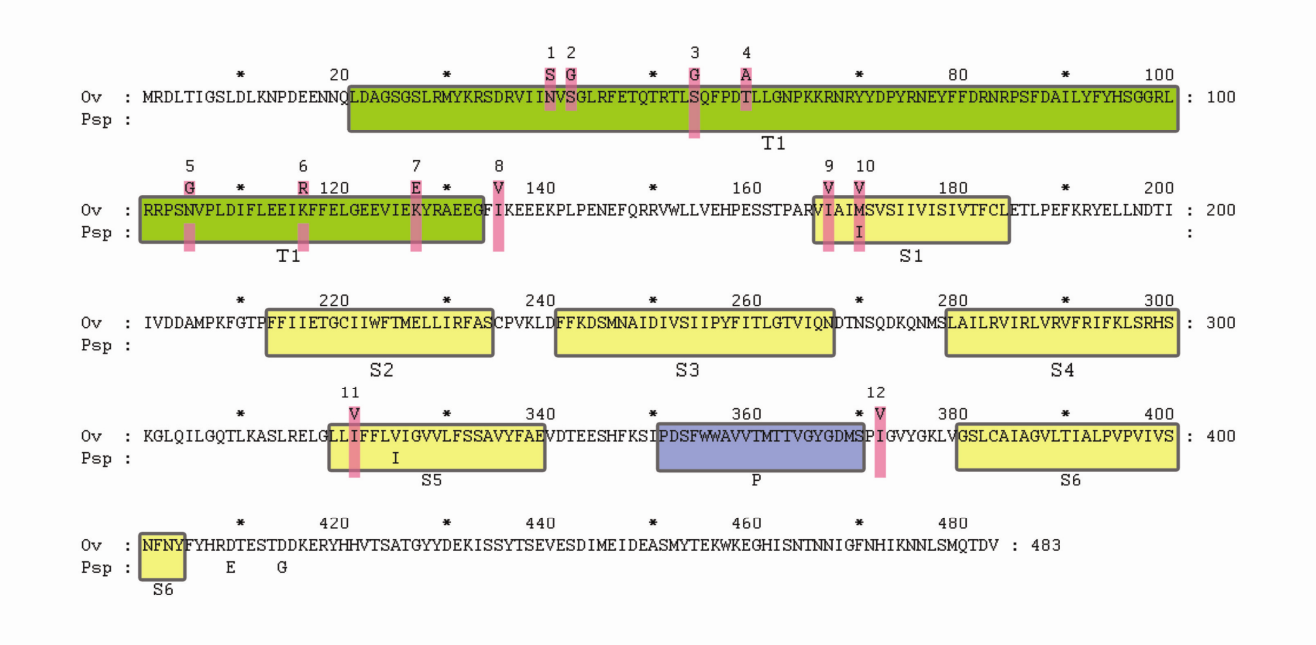

Figure S1. Map of Kv1.1 channels with editing sites for a tropical and an Antarctic octopus. Amino acid sequence alignment for the tropical (*Octopus vulgaris*) and Antarctic (*Pareledone* sp.) octopus K_v1 channels. For *Pareledone* sp. only genomic-level amino acid differences are shown. Codons containing editing sites are highlighted in pink. The amino acid changes caused by editing are listed above the edited position. Numbers refer to editing sites listed in Figure 2A.

Fig. S2

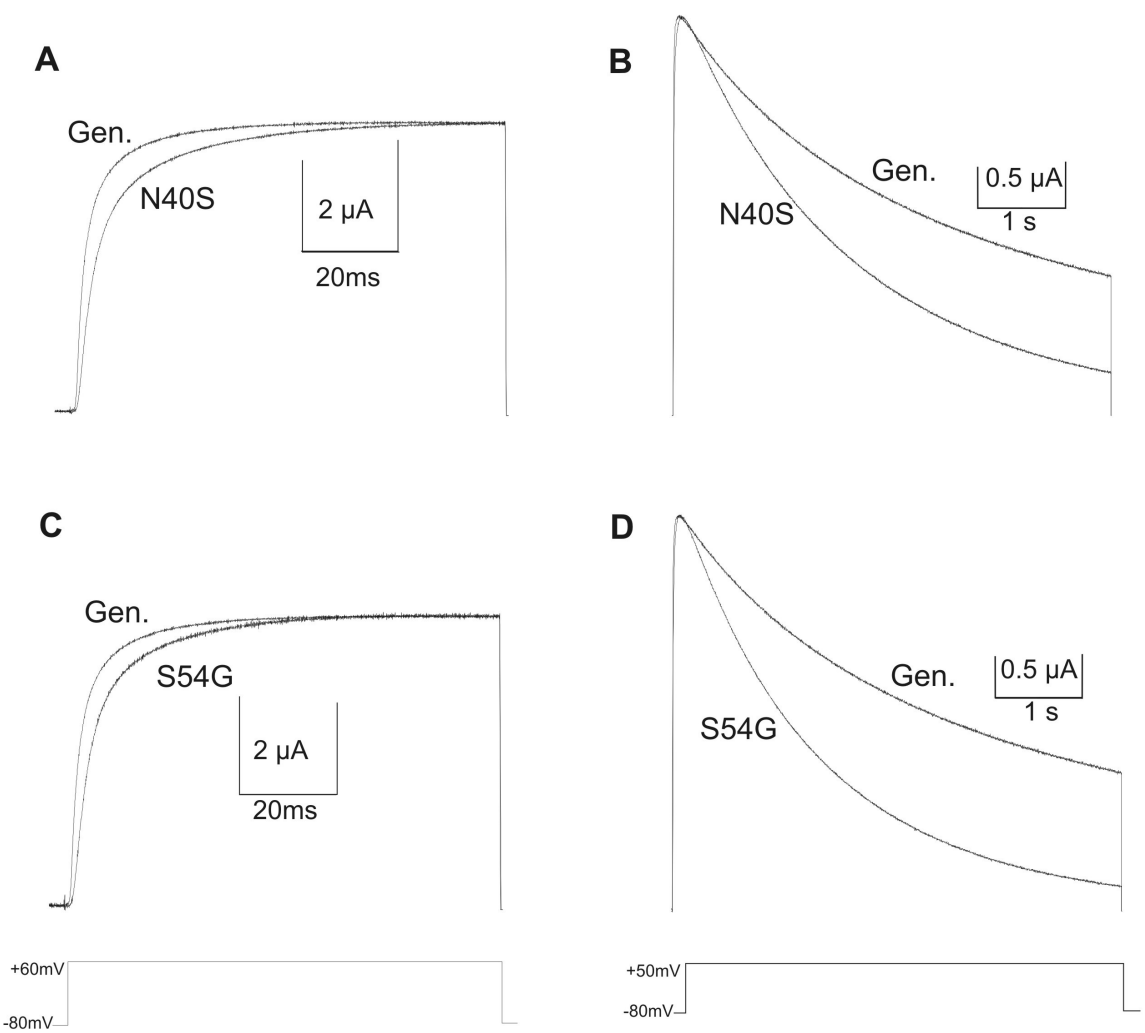

Figure S2. Two tropical editing sites change opening and inactivation kinetics. A and **B**, representative overlapping current traces for the genomic tropical (*Octopus vulgaris*) and the same channel containing the N40S edit. Panel **A** shows traces following a voltage step from -80 mV to +60 MV recorded at a fast sampling rate in order to compare activation kinetics. Panel **B** show traces following a voltage step from -80 mV to +50 mV recorded at a slow sampling rate to compare inactivation kinetics. Panels **C** and **D** are the same as from **A** and **B** except with the S54G edit instead of N40S. Experiments were conducted at 15°C. Both edits significantly slow opening kinetics and speed inactivation kinetics (see also Table S1).

Fig. S3

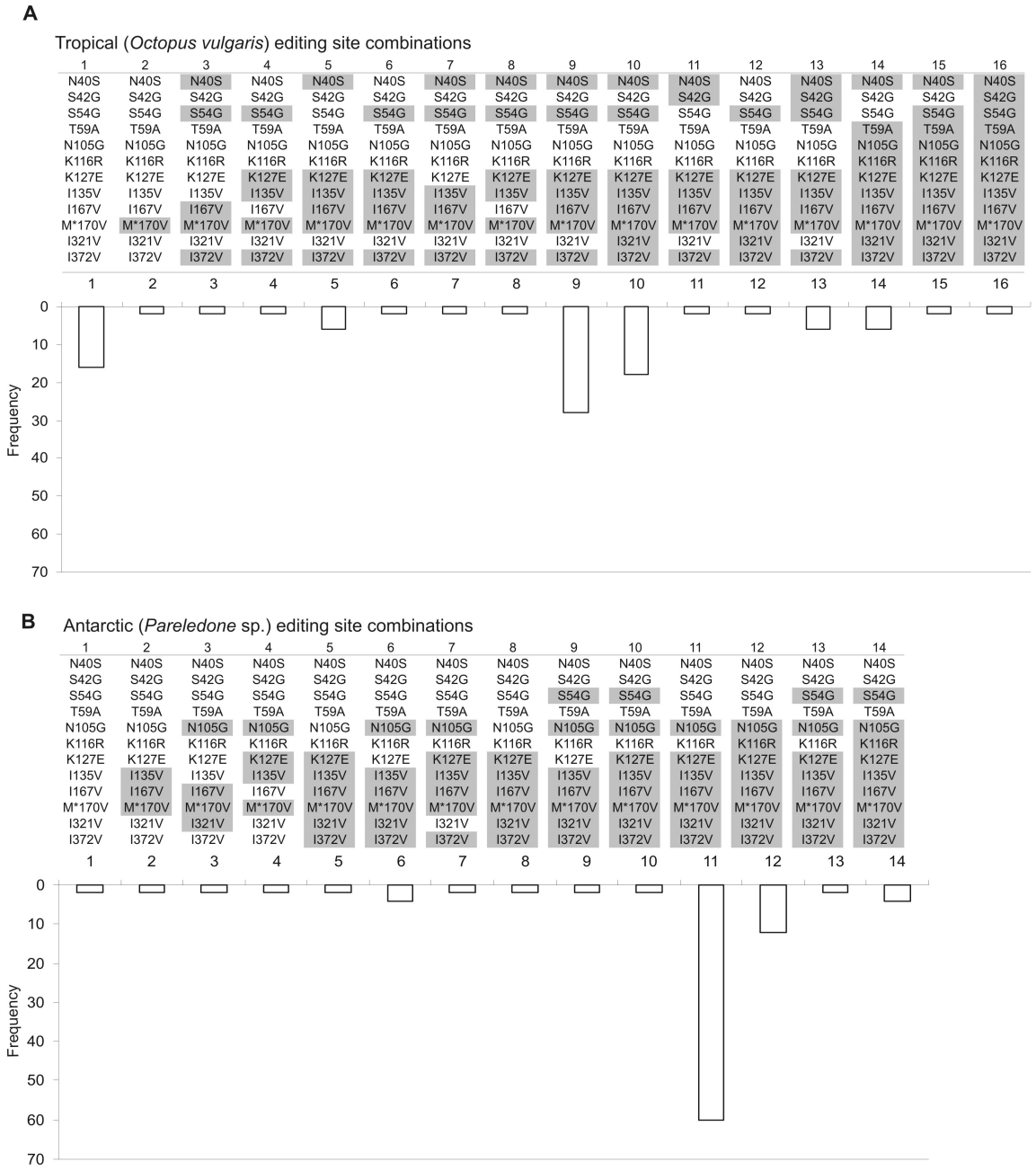

Figure S3. Octopus Kv1 channel mRNA's contain combinations of editing sites. Editing site combinations for *Pareledone* sp. (A) and *Octopus vulgaris* (B) were identified by amplifying the K_v1 channel from stellate ganglia cDNA and sequencing 50 clones. Shading means that a particular pattern contains that editing site.

Table S1.

Table S1. Functional properties of edited and unedited octopus Kv1.1 channels

	Kv1.1 construct	Temp. (°C)	$V_{1/2}$ (mV)	Z	T1/2 (ms)	Q10	Deactivation (1/s)	Q10	Inactivation tau (s)	Q10
Genomic	*Pareledone* sp	2	-16.5 ± 1.2 (6)	3.2 ± 0.24 (6)	22.5 ± 3.33 (6)	5	7.95 ± 0.47 (6)		6.39 ± 1.12 (6)	
		15	-6.1 ± 1.0 (11)	2.1 ± 0.09 (11)	2.79 ± 0.2 (11)	2.4	145 ± 7 (16)	4.2	3 ± 0.17 (12)	1.7
		25	-1.5 ± 0.6 (12)	1.9 ± 0.07(12)	1.17 ± 0.06 (12)	-	610 ± 30 (9)	-	1.76 ± 0.15 (10)	-
	O. vulgaris	2	-13.6 ± 1.2 (6)	3.2 ± 0.16 (6)	24.8 ± 4.81 (6)	4.6	6.9 ± 0.52 (6)	10.5	4.93 ± 0.99 (6)	1.6
		15	-4.9 ± 0.8 (10)	2.6 ± 0.1 (10)**	3.42 ± 0.27 (10)	2.4	146 ± 11 (9)	4	2.58 ± 0.16 (10)	1.6
		25	-2.4 ± 1.2 (9)	2.2 ± 0.09 (9)*	1.42 ± 0.10 (9)*	-	589 ± 22 (6)	-	1.62 ± 0.14 (9)	-
Single edits	I321V	15	5.2 ± 0.5 (10)***	1.8 ± 0.06 (10)*	3.06 ± 0.2 (10)	2.4	353 ± 7 (9)***	4	4.21 ± 0.34 (9)**	2.0
		25	8.3 ± 1.2 (9)***	1.8 ± 0.07 (9)	1.26 ± 0.06 (9)	-	1423 ± 99 (8)***	-	2.12 ± 0.22 (10)	-
	N105G	15	-2.3 ± 1.0 (9)*	2.3 ± 0.07 (9)	3.74 ± 0.22 (9)**	2.9	169 ± 6 (8)*	4.9	2.99 0.18 (7)	1.5
		25	4.4 ± 1.9 (8)**	2.0 ± 0.08 (8)	1.28 ± 0.04 (8)	-	832 ± 30 (8)***	-	1.94 0.07 (8)	-
	N40S	15	-1.9 ± 0.9 (10)	2.7 ± 0.18 (10)	5.21 ± 0.28 (10)***	3.6	179 ± 5 (10)*	4.3	1.98 ± 0.12 (11)**	2.0
		25	-3.2 ± 1.2 (10)	2.4 ± 0.07 (10)	1.46 ± 0.04 (10)	-	760 ± 28 (10)***	-	1.01 ± 0.04 (10)***	-
	S54G	15	-6.0 ± 0.7 (11)	3.2 ± 0.08 (11)***	5.17 ± 0.13 (11)***	3.3	199 ± 7 (11)***	2.9	1.61 ± 0.05 (11)***	1.8
		25	-2.1 ± 1.3 (12)	2.3 ± 0.03 (12)	1.59 ± 0.02 (12)	-	773 ± 22 (12)***	-	0.9 ± 0.02 (12)***	-
	Pareledone EP1	15	-1.04 ± 0.75 (12)***	1.89 ± 0.03 (12)*	2.97 ± 0.17 (12)	2.7	228 ± 2.9 (13)***	4.6	2.3 ± 0.14 (12)**	1.7
		25	4.83 ± 0.92 (10)***	1.63 ± 0.03 (10)**	1.11 ± 0.02 (9)		1059 ± 16 (9)***		1.34 ± 0.06 (9)*	
Multiple edit combinations	Pareledone EP0 (EP1 - I321V)	15	-12.3 ± 0.8 (6)***	2.78 ± 0.14 (6)***	3.25 ± 0.20 (6)		94.9 ± 3.9 (6)***		1.92 ± 0.25 (6)**	
	O. vulgaris EP1	15	-13.8 ± 0.85 (9)***	3.06 ± 0.25 (9)**	3.38 ± 0.23 (9)	3	86.8 ± 5 (8)***	5.4	1.77 ± 0.13 (11)**	1.8
		25	-7.59 ± 1.24 (7)**	2.42 ± 0.12 (7)	1.13 ± 0.06 (7)*		470 ± 27 (7)**		0.98 ± 0.05 (11)***	

V1/2 refers to the midpoint voltages for activation determined from fits of the conductance-voltage relationship to a Boltzmann function (see methods). Z refers to the steepness factor from the same fits. T1/2 refers to the time required for half maximal current measure at +60 mV. Deactivation rates were derived from time constants measured from single exponential fits to tail currents recorded at -80 mV. Inactivation tau refers to the time constant for a single exponential fit of the inactivating current measured at +50 mV. Multiple edit combinations refer to the most prevalent naturally occurring editing patterns (EP) for each species (see Figure S3). Statistical comparisons using a two-tailed t-test were made between the following: *Pareledone* sp. and *O. vulgaris* genomic channels, channels with a single editing site and their respective genomic background, between Psp EP11 and Psp genomic, between Ov EP9 and Ov genomic, and between PspEP0 and PspEP11.
*P<0.05, **P<0.01, ***P<0.001

Table S2.

Table S2. Editing of Kv1 in eight octopus species

Amino acid change	Nuc #	Domain	Editing percentages							
			O. digueti	*O. defilippi*	*O. vulgaris*	*O. bimaculata*	*O. rubescens*	*B. arcticus*	*B. piscatorum*	*Pareledone sp.*
N40S	119	T1	50	45	76	27	32	24		
S42G	124	T1			10					
S54G	160	T1	60	71	68	59	66	50	26	10
T59A	175	T1			10					
N105G-1	314	T1						39		92
N105G-2	315		10				62	89	50	92
K116R	348	T1								16
K127-1	379	T1	44	61	78	55	88	83	82	88
K127-2	380		4							
I135V	403	T1-S1 linker	66	76	80	64	94	100	89	96
I167V	499	S1	68	71	78	55	100	100	80	96
I169M	507	S1						24		
M*170V	508	S1	68	79	84	64	100	85	66	98
K274E-1	820	S3-S4 linker						71		
K274E-2	821							77		
I321V	961	S5	12	30	30	33	66	80	67	92
I372V	1114	P-S6 linker	70	83	82	70	100	97	80	90
D415G	1241	C-term	56			33	63	50	65	genomic**
Y436C	1307	C-term	8							

Editing site for *Pareledone* sp., *Octopus vulgaris*, and *Octopus digueti* were identified by sequencing 50 cDNA clones. Editing sites for the other five species were identified by directly sequencing PCR products from both stellate ganglia cDNA and genomic DNA. Editing percentages were calculated by measuring peak heights on electropherograms.
*this residue is an isoleucine in *Pareledone* sp., and a methionine in the other species; editing results in valine in both cases
**this is not an editing site in *Pareledone* sp.; glycine is the genomically encoded amino acid

Table S3

Table S3. Oligonucleotide primers

Number	Primer	Orientation	Sequence
1	Degenerate Kv1	F	GAYCCAYTAMGNAAYGARTAYTTYTTYGA
2	Degenerate Kv1	R	RTGRTARAARTARTTRAARAT
3	Degenerate Kv1, nested	R	GTCATNSWNACNACNGCCCACCA
4	5' RACE	R	CTGGATGCTCAACCAGTAGCCACACACG
5	5' RACE nested	R	CCAATTTCACAGGACAGGAAGCGAAACG
6	3' RACE	F	CTGTCACGTCATTCCAAAGGGCTTCAAA
7	3' RACE nested	F	TGGCGTTGTGTTGTTCTCCAGTGCGG
8	full length Kv1 Pareledone	F	GGATCGACATTTGTTTTTACAAGCCG
9	full length Kv1 Pareledone	R	CATCTTCTTTAAACAGCAAACTTCATATTTC
10	full length Kv1 O. vulgaris	F	GGTTTTCATTTGAAGCTGATTAAAAGATG
11	full length Kv1 O. vulgaris	R	AAACAGCAAACTCCATATTTCATAC
12	full length Kv1 O. digueti	F	GGGGTTTCATTTGAAACAGATTAAAAG
13	full length Kv1 O. digueti	R	CTCCATCTTCTTATAATTAGCAAACTCT
14	Kv1 ORF genomic	F	TCTCTGGACTTAAAAAACCCGGATG
15	All octopus expression	F	GGAGATCTACCATGAGGGATTTAACAATCGG
16	Pareledone expression	R	GGAGATCTTCATACATCAGTCTGCATGCTTAG
17	All other octopus expression	R	GGAGATCTTCATACATCAGTTTGCATGCTTAG
18	PPE assay, Pareledone	R	AGAACAACACAACGCCAATGAT
19	PPE assay, all other octopus	R	AGAACAACACAACGCCAATGAC
20	ORF Kv1 all octopus	F	RRATGAGGGATTTAACAATCGGG
21	ORF Kv1 all octopus	R	TTATTTTTGATRTGATTAAACCC

Oligonucleotide primers used in this study. Sequences are given following IUPAC code.

References and Notes

1. A. L. Hodgkin, B. Katz, The effect of temperature on the electrical activity of the giant axon of the squid. *J. Physiol.* **109**, 240 (1949). Medline

2. A. L. Hodgkin, A. F. Huxley, Currents carried by sodium and potassium ions through the membrane of the giant axon of Loligo. *J. Physiol.* **116**, 449 (1952). Medline

3. C. M. Armstrong, F. Bezanilla, E. Rojas, Destruction of sodium conductance inactivation in squid axons perfused with pronase. *J. Gen. Physiol.* **62**, 375 (1973). doi:10.1085/jgp.62.4.375 Medline

4. F. Kukita, Properties of sodium and potassium channels of the squid giant axon far below 0 degrees C. *J. Membr. Biol.* **68**, 151 (1982). doi:10.1007/BF01872261 Medline

5. B. M. Rodríguez, D. Sigg, F. Bezanilla, Voltage gating of Shaker K+ channels. The effect of temperature on ionic and gating currents. *J. Gen. Physiol.* **112**, 223 (1998). doi:10.1085/jgp.112.2.223 Medline

6. Materials and methods are available as supporting material on *Science* Online.

7. M. E. Katz *et al.*, Impact of Antarctic Circumpolar Current Development on Late Paleogene Ocean Structure. *Science* **332**, 1076 (2010). doi:10.1126/science.1202122

8. J. J. Rosenthal, R. G. Vickery, W. F. Gilly, Molecular identification of SqKv1A. A candidate for the delayed rectifier K channel in squid giant axon. *J. Gen. Physiol.* **108**, 207 (1996). doi:10.1085/jgp.108.3.207 Medline

9. B. L. Bass, H. Weintraub, An unwinding activity that covalently modifies its double-stranded RNA substrate. *Cell* **55**, 1089 (1988). doi:10.1016/0092-8674(88)90253-X Medline

10. C. Basilio, A. J. Wahba, P. Lengyel, J. F. Speyer, S. Ochoa, Synthetic polynucleotides and the amino acid code. V. *Proc. Natl. Acad. Sci. U.S.A.* **48**, 613 (1962). doi:10.1073/pnas.48.4.613 Medline

11. T. Bhalla, J. J. Rosenthal, M. Holmgren, R. Reenan, Control of human potassium channel inactivation by editing of a small mRNA hairpin. *Nat. Struct. Mol. Biol.* **11**, 950 (2004). doi:10.1038/nsmb825 Medline

12. C. M. Burns *et al.*, Regulation of serotonin-2C receptor G-protein coupling by RNA editing. *Nature* **387**, 303 (1997). doi:10.1038/387303a0 Medline

13. T. Melcher, S. Maas, M. Higuchi, W. Keller, P. H. Seeburg, Editing of alpha-amino-3-hydroxy-5-methylisoxazole-4-propionic acid receptor GluR-B pre-mRNA in vitro reveals site-selective adenosine to inosine conversion. *J. Biol. Chem.* **270**, 8566 (1995). doi:10.1074/jbc.270.15.8566 Medline

14. D. E. Patton, T. Silva, F. Bezanilla, RNA editing generates a diverse array of transcripts encoding squid Kv2 K+ channels with altered functional properties. *Neuron* **19**, 711 (1997). doi:10.1016/S0896-6273(00)80383-9 Medline

15. J. J. Rosenthal, F. Bezanilla, Extensive editing of mRNAs for the squid delayed rectifier K+ channel regulates subunit tetramerization. *Neuron* **34**, 743 (2002). doi:10.1016/S0896-6273(02)00701-8 Medline

16. S. B. Long, E. B. Campbell, R. Mackinnon, Crystal structure of a mammalian voltage-dependent Shaker family K+ channel. *Science* **309**, 897 (2005). doi:10.1126/science.1116269 Medline

17. A. Kreusch, P. J. Pfaffinger, C. F. Stevens, S. Choe, Crystal structure of the tetramerization domain of the Shaker potassium channel. *Nature* **392**, 945 (1998). doi:10.1038/31978 Medline

18. M. Li, Y. N. Jan, L. Y. Jan, Specification of subunit assembly by the hydrophilic amino-terminal domain of the Shaker potassium channel. *Science* **257**, 1225 (1992). doi:10.1126/science.1519059 Medline

19. W. R. Kobertz, C. Williams, C. Miller, Hanging gondola structure of the T1 domain in a voltage-gated K(+) channel. *Biochemistry* **39**, 10347 (2000). doi:10.1021/bi001292j Medline

20. S. J. Cushman *et al*., Voltage dependent activation of potassium channels is coupled to T1 domain structure. *Nat. Struct. Biol.* **7**, 403 (2000). doi:10.1038/75185 Medline

21. D. L. Minor, Jr. *et al*., The polar T1 interface is linked to conformational changes that open the voltage-gated potassium channel. *Cell* **102**, 657 (2000). doi:10.1016/S0092-8674(00)00088-X Medline

22. Z. Lu, A. M. Klem, Y. Ramu, Coupling between voltage sensors and activation gate in voltage-gated K+ channels. *J. Gen. Physiol.* **120**, 663 (2002). doi:10.1085/jgp.20028696 Medline

23. G. J. Soler-Llavina, T. H. Chang, K. J. Swartz, Functional interactions at the interface between voltage-sensing and pore domains in the Shaker K(v) channel. *Neuron* **52**, 623 (2006). doi:10.1016/j.neuron.2006.10.005 Medline

24. S. B. Long, X. Tao, E. B. Campbell, R. MacKinnon, Atomic structure of a voltage-dependent K+ channel in a lipid membrane-like environment. *Nature* **450**, 376 (2007). doi:10.1038/nature06265 Medline

25. M. M. Pathak *et al*., Closing in on the resting state of the Shaker K(+) channel. *Neuron* **56**, 124 (2007). doi:10.1016/j.neuron.2007.09.023 Medline

26. F. Conti, E. Neher, Single channel recordings of K+ currents in squid axons. *Nature* **285**, 140 (1980). doi:10.1038/285140a0 Medline

27. I. Llano, C. K. Webb, F. Bezanilla, Potassium conductance of the squid giant axon. Single-channel studies. *J. Gen. Physiol.* **92**, 179 (1988). doi:10.1085/jgp.92.2.179 Medline

28. F. Qin, L. Li, Model-based fitting of single-channel dwell-time distributions. *Biophys. J.* **87**, 1657 (2004). doi:10.1529/biophysj.103.037531 Medline

29. B. R. Graveley *et al*., The developmental transcriptome of Drosophila melanogaster. *Nature* **471**, 473 (2011). doi:10.1038/nature09715 Medline

30. H. Lomeli *et al*., Control of kinetic properties of AMPA receptor channels by nuclear RNA editing. *Science* **266**, 1709 (1994). doi:10.1126/science.7992055 Medline

31. R. A. Reenan, Molecular determinants and guided evolution of species-specific RNA editing. *Nature* **434**, 410 (2005). doi:10.1038/nature03364

32. E. R. Liman, J. Tytgat, P. Hess, Subunit stoichiometry of a mammalian K+ channel determined by construction of multimeric cDNAs. *Neuron* **9**, 861 (1992). doi:10.1016/0896-6273(92)90239-A Medline

33. M. Taglialatela, L. Toro, E. Stefani, Novel voltage clamp to record small, fast currents from ion channels expressed in Xenopus oocytes. *Biophys. J.* **61**, 78 (1992). doi:10.1016/S0006-3495(92)81817-9 Medline

34. L. S. Milescu, G. Akk, F. Sachs, Maximum likelihood estimation of ion channel kinetics from macroscopic currents. *Biophys. J.* **88**, 2494 (2005). doi:10.1529/biophysj.104.053256 Medline

35. L. M. Roberson, J. J. Rosenthal, An accurate fluorescent assay for quantifying the extent of RNA editing. *RNA* **12**, 1907 (2006). doi:10.1261/rna.166906 Medline